

The Relationship between the Fatigue Strength Coefficient
and the Three Dimensional State of Stress at a Hole

Yao Weixing

Mechanical Engineering Dept., Tsinghua University
Beijing, PRC

Yang Qingxiong

Aircraft Dept., Northwestern Polytechnical University
Xi'an, Shaanxi Province, PRC

Third International Conference on Biaxial/Multiaxial Fatigue,
April 3-6, 1989 Stuttgart, FRG

Abstract

In this paper the main causes of differences between the fatigue strength coefficient K_f and the theoretical stress concentration coefficient K_t are discussed, and the effects of three dimensional state of stress and the stress gradient at a hole on K_f are also investigated using a micromechanics model. A formula to predict K_f is obtained based on the model of fatigue nucleation postulated by Wood. This formula indicates that under high cycle fatigue conditions the stress gradient has almost no effect on K_f , but the three dimensional stress and the smooth specimen size determine the difference between K_f and K_t . From this formula, it can be deduced that K_f will increase as the cycles to failure increase for cyclic hardening materials, on the contrary, K_f will decrease as the cycles to failure increase for cyclic softening materials. This deduction has been checked by experiments on cyclic hardening materials Ly12-cs and Ly12B-az Al alloys. An example of predicting K_f for a plane with a hole is also given in this paper.

Introduction

The mechanism of fatigue nucleation has been investigated widely and the results of investigation indicate that fatigue nucleation is caused by the plastic deformation accumulated with

the increase of fatigue cycles^{/1,2/}. There are many models^{/1-4/} to describe this mechanism and among the models, the extrusion and intrusion model postulated by Wood^{/3/} is popularly accepted now.

There are two sources of local plasticity. One is the external, for example, the stress concentration caused by notches, etc.. The other is the internal, that is, the scatter of the material structures.

In general, the fatigue strength coefficient K_f is substituted for theoretical stress concentration coefficient K_t in the local strain method of predicting the fatigue life, to take the three dimensional stress and stress gradient at a notch into consideration. K_f can be defined as follows,

$$K_f = \frac{\text{the fatigue strength of smooth specimens at one fatigue life}}{\text{the fatigue strength of notched specimens at the same fatigue life}} \quad (1)$$

Obviously K_f is a function of fatigue life. There are many formulae to estimate K_f , and among which the Neuber's and Peterson's are well-known and widely employed today^{/5/}, but all these estimations didn't consider the effect of the fatigue life on K_f .

In this paper the main causes of differences between K_f and K_t are discussed. According to the above definition, a formula to estimate K_f is presented and from this formula some important results are deduced and checked. An example of predicting K_f is also given to show that the estimation is not complicated and the methodology has a adaptability.

Computational Micromechanics Model

The computational micromechanics model which was given by one of the authors^{/6/} is one of the micromechanics models, in order to provide a new approach to quantitative analysis of the mechanical behaviour of engineering materials in consideration of microstructures. This model deems that materials have a microstructure, all of the field quantities are random variables or statistic functions, and all features which break the homogeneity and continuity of the material structure are called "defects" which play an important role in the behaviour of materials.

Based on the above basic hypotheses, reference /6/ defines and discusses the computational micromechanics model, reviews and studies the fundamental theories adapted to this model, presents the transition function method to obtain the relations between macroscopic and microscopic quantities, and gives the general steps of solving problems. Here only briefly reviews the steps to analyze a mechanical behaviour of metal: (1) the preparation of the microstructure datum. If these datum are not available, some experiments on the microscopic properties of the material should be done. These datum usually include the compositions of the material, the percentage and the distribution of each composition, the main defects of the material, etc., (2) according to the problem to be solved, an interested local domain which is rather smaller than the specimen but much larger than microscopic scale is separated from the specimen in order to reduce the numbers of elements in numerical analysis. The loads acted on the local domain can be easily computed using macro-mechanics (Fig.1), (3) then based on the experimental datum, the local domain is separated using Monte Carlo Method, (4) the microscopic parameters, such as voids, dislocations, etc., are introduced into the numerical or theoretical analysis. What microscopic parameters are introduced depends on the micromechanism of the mechanical behaviour concerned, which usually have been investigated, (5) summarize the theoretical and numerical results.

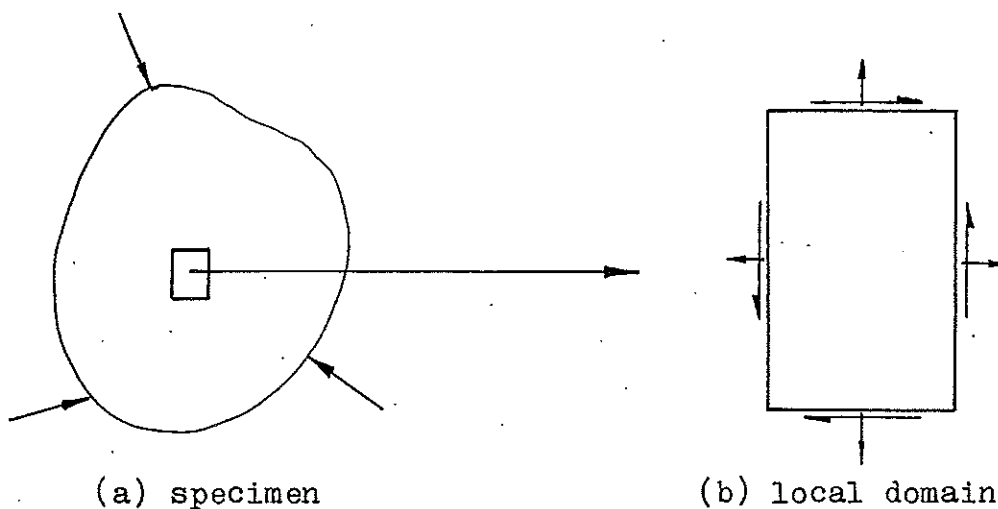


Fig.1 The local domain

Estimation of K_f

1. Crack nucleation model

Under high cycle fatigue, the fatigue crack nucleation can be described by the extrusion and intrusion model postulated by Wood, and the dislocation dipole model has successfully explained the ratcheting phenomena of fatigue^{/7/}, Fig.2.

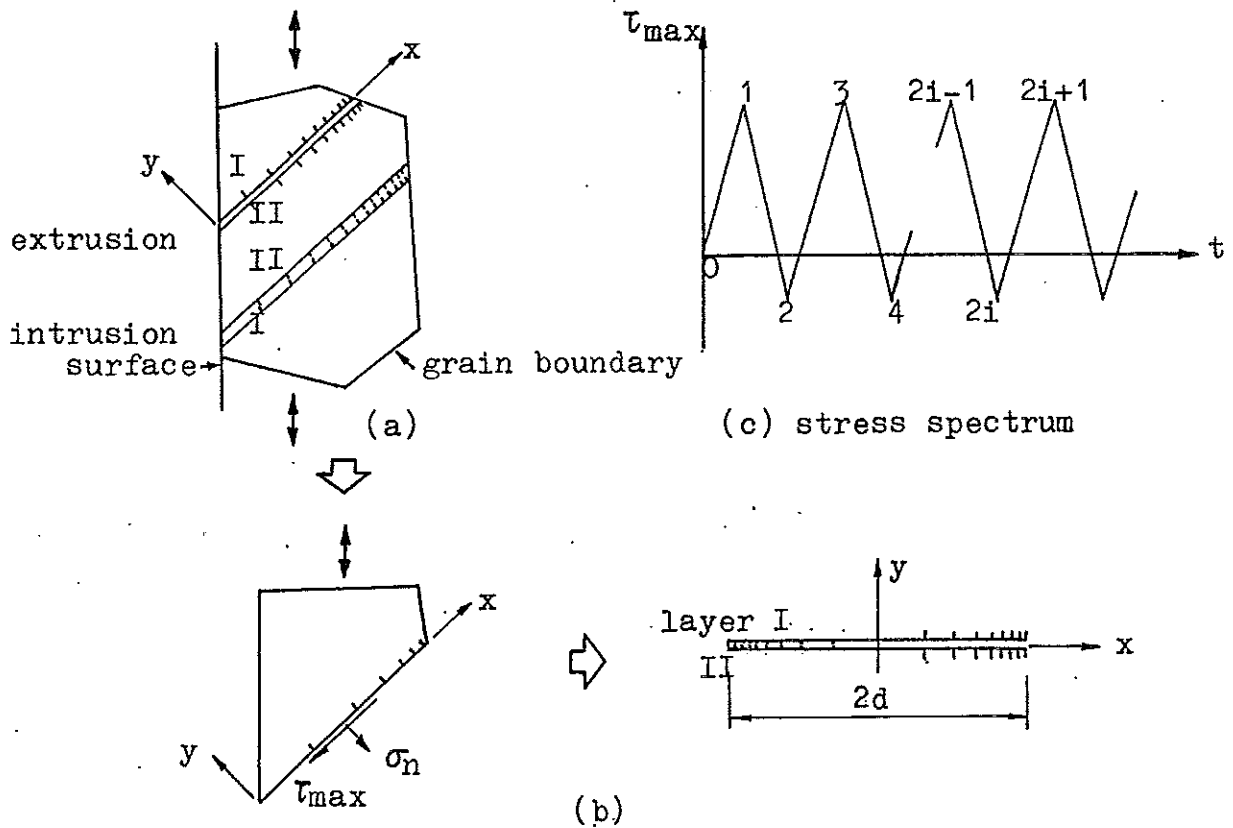


Fig.2 The model of fatigue crack nucleation

A smooth specimen is under a cyclic uniaxial loading. During the first loading, a slip takes place along a line(layer I) inclined by 45° against the axis of the loading. Dislocations are piled up on layer I. For the unloading, a reversal slip takes place on a line(layer II) located close to the layer I. Dislocations with the opposite sign are piled up on the layer II, and in each of the following loadings, more positive dislocations are piled up on layer I, and in each of the following unloadings, more negative dislocations are piled up on layer II, and both the dislocations are piled up against a grain boundary. Since the plas-

tic deformation is irreversible, the dislocation density on layer I is not changed during the unloading and that on layer II is not influenced by the loading. The dislocation density $D(x)$ can be solved using the method given by Leibried^{/8/} for the model as shown in Fig.2(b). The self elastic strain energy of the accumulated dislocations U can also be obtained,

$$D(x) = \pm \frac{(\Delta\tau - 2k)}{\pi A} \frac{x}{(d^2 - x^2)^{1/2}} \quad (2)$$

$$U = \frac{(\Delta\tau - 2k)^2}{8A} d^2 i \quad (3)$$

where positive sign in equation (2) is taken for layer I, and the negative sign for layer II, k is the friction stress, d is the grain size, $A = G/2\pi(1-\nu)$ for edge dislocations, $A = G/2\pi$ for screw dislocations, G is the shear modulus and ν is Poisson's ratio. The dislocations monotonically increase as the cycles increase. Physically, it is impossible to have an infinite number of dislocations in the material. So a criterion for the fatigue crack initiation could be a critical value of U ,

$$U = W_c d \quad (4)$$

where W_c is the specific fracture energy for a unit area and is a material constant. From equations (3) and (4), it can be obtained

$$8AW_c = (\Delta\tau - 2k)^2 n d \quad (5)$$

where n is the cycles to nucleate.

2. Crack initiation at a notch root

Based on the computational micromechanics model as stated above, it is not difficult to find the most dangerous element at a notch root. Usually this element is in three dimensional state of stress as shown in fig.3(a). From this the maximum shear stress and the normal stress can be obtained easily,

$$\begin{aligned} \sigma_n &= \sigma_n(x) \\ \tau &= \tau(x) \end{aligned} \quad (6)$$

$\sigma_n(x)$ and $\tau(x)$ vary with the geometry, external load, microstruc-

ture of the material, etc.. For a small x , equation (6) can be approximated as

$$\begin{aligned}\sigma_n &= \sigma_0 - C_\sigma x \\ \tau &= \tau_0 - C_\tau x\end{aligned}\quad (7)$$

where C_σ and C_τ are the gradients of normal stress and shear stress at the root of a notch respectively, σ_0 and τ_0 are the normal stress and shear stress at the edge of the notch.

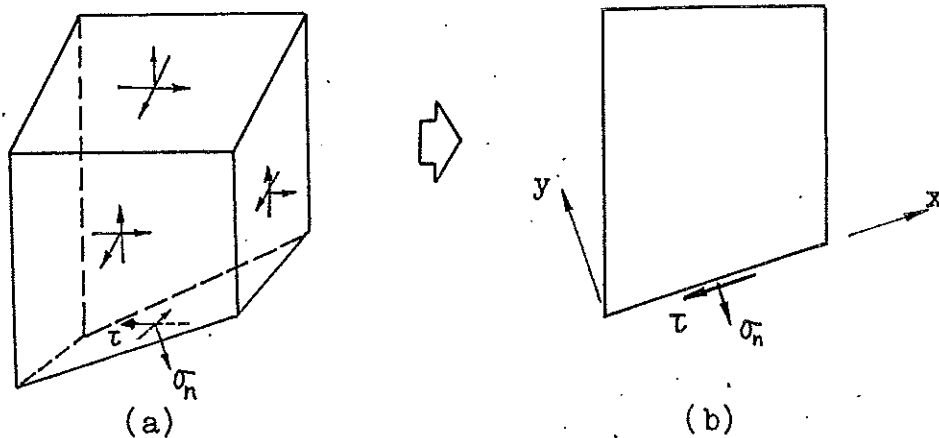


Fig.3 Three dimensional stress state of an element at the notch root

The dislocation density $D_n(x)$ and the self elastic strain energy U_n can be obtained as the above section,

$$D_n(x) = \pm \frac{(\Delta\tau_0 - C_\tau x - 2k)}{\pi A} \cdot \frac{x i}{(d^2 - x^2)^{1/2}} \pm \frac{C_\tau}{2\pi A} \cdot \frac{d i}{(d^2 - x^2)^{1/2}} \quad (8)$$

$$U_n = \frac{1}{8A} (\Delta\tau_0 - 2k)^2 d^2 - \frac{1}{4\pi A} (\Delta\tau_0 - 2k) C_\tau d^3 + \frac{1}{64A} C_\tau^2 d^4 \quad (9)$$

When $U_n = W_c d$, the crack initiated, and then equation (9) can be written as

$$8AW_c = n(\Delta\tau_0 - 2k)^2 d - \frac{2n}{\pi} (\Delta\tau_0 - 2k) C_\tau d^2 + \frac{n}{8} C_\tau^2 d^3 \quad (10)$$

To compare eq. (5) with eq. (10), there is influence of two behind terms in equation (10) on the crack initiation when the stress gradient is considered.

3. Estimation of K_f

From equation (5), the relationship between the load $\Delta\tau$ and the fatigue life n of the crack initiation can be written as

$$\Delta\tau = 2k + \sqrt{\frac{8AW_c}{nd}} \quad (11)$$

When the material microstructure enters in consideration, the external gross stress $\Delta\tau_g$ is different from the internal stress $\Delta\tau$ acted on the most serious element. Suppose

$$\Delta\tau = K_\sigma \cdot \Delta\tau_g \quad (12)$$

where K_σ is called as microstress concentration coefficient of a smooth specimen, and K_σ is equal to 1 for homogeneous materials. When equation (12) is used, (11) is written as

$$K_\sigma \cdot \Delta\tau_g = 2k + \sqrt{\frac{8AW_c}{nd}} \quad (13)$$

Similarly, for a notched specimen, we can solve eq.(10)

$$\Delta\tau_o \doteq 2k + \frac{C_t d}{\pi} + \sqrt{\frac{8AW_c}{nd}} \quad (14)$$

and let K_σ^n be the microstress concentration coefficient of a notched specimen, then

$$\Delta\tau_o = K_\sigma^n \cdot \Delta\tau_g^n \quad (15)$$

Obviously, K_σ^n is equal to K_t under conditions of linear elastic stress and homogeneous materials. When eq.(15) is used, eq.(14) is written as

$$K_\sigma^n \cdot \Delta\tau_g^n = 2k + \frac{C_t d}{\pi} + \sqrt{\frac{8AW_c}{nd}} \quad (16)$$

According to the definition of K_f eq.(1), the following formula can be obtained from equations (13) and (16),

$$\begin{aligned} K_f &= \Delta\tau_g / \Delta\tau_g^n \\ &= \frac{K_\sigma^n}{K_\sigma} \left(1 - \frac{C_t d}{2\pi k + C_t d + \pi \sqrt{\frac{8AW_c}{nd}}} \right) \end{aligned} \quad (17)$$

The formula (17) gives an estimation of the fatigue stress coefficient K_f . From this formula it can be seen that K_f is related

to fatigue life n , the size of specimens (K_{σ}^n, K_{σ}), the geometry of the notch (K_{σ}^n, C_t), the material (d, W_c, A , etc.), and so on. From this formula, the following two results can be deduced.

(a) In general, $C_t d \ll 2\pi k$, so the above equation (17) can be written as follows

$$K_f = K_{\sigma}^n / K_{\sigma} \quad (18)$$

that is to say, under high cycle fatigue conditions, stress gradient has almost no effect on K_f , but the three dimensional state of stress at a notch and the smooth specimen size determine the difference between K_f and K_t .

(b) In high cycle fatigue, the root of the notch is in elasticity during cyclic loading, so K_{σ}^n is a constant and then K_f is expected to be a constant. But if the root of a notch is under elasto-plasticity, K_{σ}^n will increase as the cycles to failure increase for cyclic hardening materials and K_{σ}^n will decrease as the cycles to failure increase for cyclic softening materials. So it can be deduced that K_f will increase as the cycles to failure increase for cyclic hardening materials, and on the contrary, K_f will decrease as the cycles to failure increase for cyclic softening materials. Fig.4 presents the experimental results of K_f for hardening material Ly12-cs and Ly12B-cz to check this deduction.

4. Estimation of K_f distribution

From the hypotheses of the computational micromechanics model stated in the above paragraph, it is known that K_{σ} and K_{σ}^n are random variables, so K_f is a random function.

Let the probabilistic density function of K_{σ} be $f(x)$, the probabilistic density function of K_{σ}^n be $f_n(y)$, then the probabilistic density function of K_f is

$$f_k(z) = \frac{d}{dz} \iint_D f(x) f_n(y) dx dy \quad (19)$$

where D is integral domain enclosed by $\frac{x}{y} \leq z$ and intervals of the random variable x value and the random variable y value.

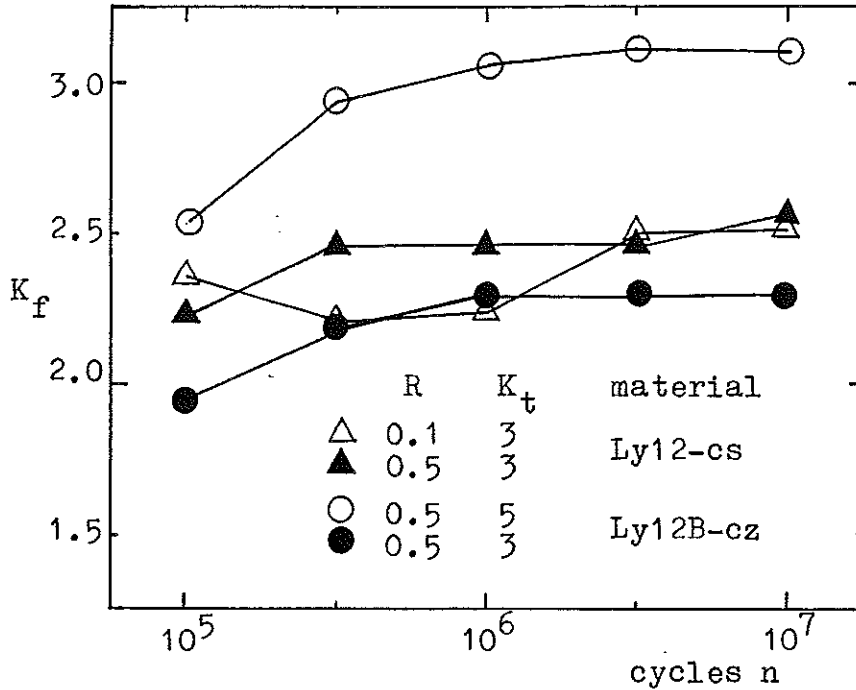


Fig.4 The experimental results of K_f of Ly12-cs and Ly12B-cz Al alloys

A Numerical Example

As a numerical example, the K_f of a plane with a central hole (Fig.5, $K_t=3.25$) is estimated. Here only gives the estimated results.

First the microstress distribution in the smooth specimen is obtained through the numerical analysis according to the computational micromechanics model. Table I presents the 45 maximum microstress values for 45 random distribution of the microstructure of the carbon steel ($\sigma_b \approx 65 \text{ kg/mm}^2$) under the gross stress $S_g = 10 \text{ kg/mm}^2$. For the datum of table I, τ_{\max} can be approximated to the shift Log-Normal distribution,

$$f(\tau_{\max}) = \begin{cases} \frac{1}{\sqrt{2\pi} \sigma_t (\tau_{\max} - \tau_0)} \exp\left(-\frac{(\ln(\tau_{\max} - \tau_0) - \tau_m)^2}{2 \sigma_t^2}\right) & \tau_{\max} \geq \tau_0 \\ 0 & \tau_{\max} < \tau_0 \end{cases} \quad (20)$$

where $\tau_0 = 0.68250$, $\tau_m = 1.66128$, $\sigma^2 = 0.012001$.

Similarity, the microstress distribution can also be computed

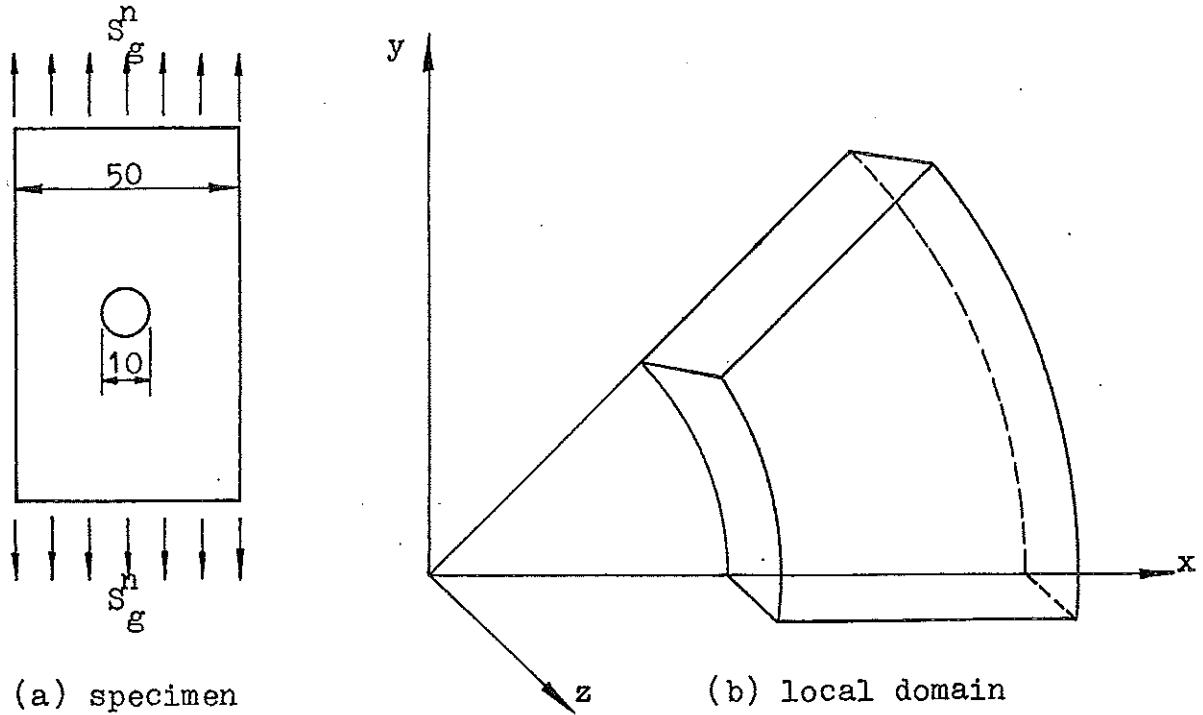


Fig.5 A specimen with a central hole

for the local domain as shown in Fig.5 under the gross stress $S_g^n = 10 \text{ kg/mm}^2$. The numerical results are listed in table II. τ_{\max} can be approximated to

$$f_n(\tau_{\max}) = \begin{cases} \frac{1}{b-a} & b \leq \tau_{\max} \leq a \\ 0 & \text{others} \end{cases} \quad (21)$$

where $a=9.58209$, $b=22.98031$.

Then using eq.(19), we can obtain the density function of K_f ,

$$f_k(z) = \begin{cases} \frac{b/z}{a/z} \int_{b-a}^t h(t) dt & 0 < z \leq a/\tau_0 \\ \frac{b/z}{\tau_0} \int_{b-a}^t h(t) dt & a/\tau_0 < z \leq b/\tau_0 \\ 0 & \text{others} \end{cases} \quad (22)$$

$$\text{where } h(t) = \frac{1}{\sqrt{2\pi}\sigma_t(t-\tau_0)} \exp\left(-\frac{(\ln(t-\tau_0) - \tau_m)^2}{2\sigma_t^2}\right)$$

The curve of $f_k(z)$ is presented in Fig.6. For eq.(22) it is calculated that the mean value of K_f is 2.748, and this value is fairly coincided with the prediction of Perterson's, $K_f \approx 2.7$.

Table I Datum of the microstress in a smooth specimen

| No. | σ_3 | σ_2 | σ_1 | τ_{max} |
|-----|------------|------------|------------|--------------|
| 1 | -1.61336 | 0.59456 | 8.73987 | 5.17662 |
| 2 | -1.60788 | 0.48199 | 8.76099 | 5.18444 |
| 3 | -1.47955 | 0.66840 | 9.00151 | 5.24053 |
| 4 | -2.00066 | 0.32291 | 8.61931 | 5.30999 |
| 5 | -0.48355 | 1.15925 | 10.28063 | 5.38209 |
| 6 | 0.52533 | 1.59127 | 11.29239 | 5.38353 |
| 7 | -1.23093 | 0.33595 | 9.60970 | 5.42031 |
| 8 | -2.09433 | 0.62894 | 8.89480 | 5.49459 |
| 9 | 0.34311 | 1.45777 | 11.39429 | 5.52559 |
| 10 | -2.05669 | 0.31895 | 9.01135 | 5.53402 |
| 11 | -2.42485 | 0.03707 | 8.64542 | 5.53513 |
| 12 | -2.94036 | 0.15362 | 8.23606 | 5.58821 |
| 13 | 0.41707 | 1.82492 | 11.62684 | 5.60488 |
| 14 | -2.51336 | -0.06750 | 8.75228 | 5.63282 |
| 15 | -0.98730 | 0.56040 | 10.31837 | 5.65283 |
| 16 | 0.39010 | 1.52939 | 11.83952 | 5.72471 |
| 17 | -0.69126 | 1.19181 | 10.80080 | 5.74603 |
| 18 | -0.89540 | 0.80998 | 10.67526 | 5.78533 |
| 19 | -0.88049 | 1.11418 | 10.70233 | 5.79141 |
| 20 | -4.30346 | -0.78936 | 7.28866 | 5.79606 |
| 21 | -0.77206 | 0.98654 | 10.84720 | 5.80963 |
| 22 | -0.92089 | 0.81311 | 10.73482 | 5.82785 |
| 23 | -2.90005 | 0.00996 | 8.87684 | 5.88845 |
| 24 | -0.87172 | 0.87893 | 10.91073 | 5.89123 |
| 25 | -2.50218 | 0.16887 | 9.32148 | 5.91183 |
| 26 | -1.97325 | 0.60859 | 9.86623 | 5.91974 |
| 27 | -0.74223 | 0.73164 | 11.13479 | 5.93851 |
| 28 | -2.88111 | -0.21423 | 9.05587 | 5.96849 |
| 29 | -3.15351 | -0.09561 | 8.78432 | 5.96891 |
| 30 | -0.78423 | 0.83183 | 11.16008 | 5.97215 |
| 31 | -2.88836 | -0.08844 | 9.13781 | 6.01309 |
| 32 | -0.98597 | 1.49865 | 11.14172 | 6.06384 |
| 33 | -1.34998 | 1.09336 | 10.77777 | 6.06388 |
| 34 | -0.60209 | 0.89191 | 11.67587 | 6.13898 |
| 35 | -2.22719 | 0.66866 | 10.39232 | 6.30976 |
| 36 | 0.49114 | 1.20563 | 13.28293 | 6.39589 |
| 37 | 0.65367 | 1.19012 | 14.60220 | 6.47427 |
| 38 | 0.20490 | 1.16288 | 13.21196 | 6.50353 |
| 39 | 0.25872 | 1.27493 | 13.83243 | 6.78685 |
| 40 | -2.298073 | 0.46153 | 10.61173 | 6.79623 |
| 41 | -3.26709 | 0.26928 | 10.40424 | 6.83567 |
| 42 | -2.68410 | 0.49842 | 11.26611 | 6.97510 |
| 43 | 0.34042 | 0.48477 | 14.52277 | 7.09117 |
| 44 | 0.75461 | 1.04370 | 15.57885 | 7.41212 |
| 45 | 0.86779 | 1.01178 | 16.16002 | 7.64611 |

Table II Datum of microstress at the root of the hole

| | | | | | |
|----------|----------|----------|----------|----------|----------|
| 9.17506 | 10.45957 | 10.60805 | 12.15397 | 12.42493 | 12.72018 |
| 12.82807 | 12.84184 | 13.47050 | 13.49480 | 14.67484 | 14.73700 |
| 15.24181 | 15.63136 | 16.22176 | 16.69189 | 16.92330 | 17.46455 |
| 17.61833 | 18.66148 | 19.42490 | 19.70090 | 19.82032 | 20.26209 |
| 21.02320 | 21.55563 | 21.89124 | 21.92070 | 22.52271 | |

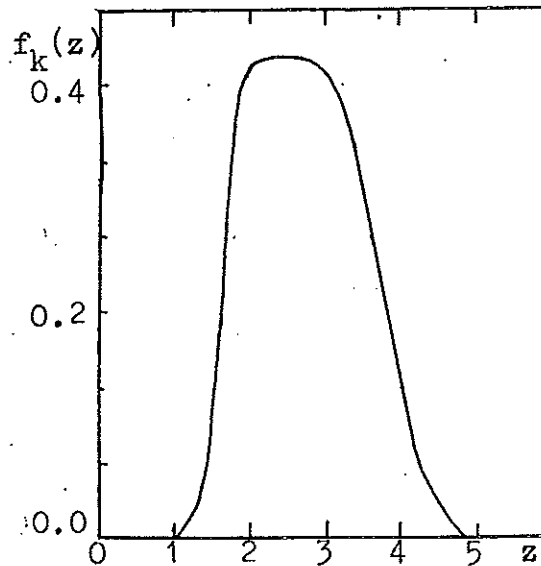


Fig.6 The probabilistic density of K_f

Conclusion

The computational micromechanics model is briefly reviewed. The main causes of the difference between K_f and K_t are discussed. A formula to estimate K_f , especially under high cycle fatigue, is given, and then the distribution of K_f is roughly investigated which is rarely studied until now. The following conclusions are derived from these results.

1. Under high cycle fatigue conditions, the stress gradient at a notch has almost no effect on K_f , but the three dimensional stress at the hole and the smooth specimen size determine the difference between K_f and K_t .
2. K_f is a statistic function which is mainly related to the material microstructure and the geometry of the notch.
3. K_f increases as the cycles to failure increase for the cyclic hardening materials, and K_f decreases as the cycles to failure increase for the cyclic softening materials.

Acknowledgement

This research is a part of the project on "research on the fatigue small cracks in metals using the micromechanics" which is supported by the chinese national fund for natural scientific research.

References

- /1/ D.Broek, Elementary Engineering Fracture Mechanics, Noordhoff International Publishing, Leyden, 1974
- /2/ A.H.Cottrell and A.J.McEvily, Fracture of Structural Materials, John Wiley, 1967
- /3/ W.A.Wood, Recent Observation on Fatigue Fracture in Metals, ASTM STP 237, 1958, pp.110-121
- /4/ T.H.Lin and Y.M.Ito, Mechanics of Fatigue Crack Nucleation, Journal of Mechanics and Physics of Solids, Vol.17, 1969, pp.511-523
- /5/ R.E.Perterson, Analytic Approach to Stress Concentration Effect in Fatigue of Aircraft Materials, Proceeding of Symposium on Fatigue of Aircraft Structures, WADC Technical Report 59-507, Aug.1959, pp.273-299
- /6/ Yao Weixing, Theory of Computational Micromechanics with applications, Ph.D. Thesis, Northwestern Polytechnical University, May 1988
- /7/ T.Mura and K.Tanaka, Dislocation Dipole Models For Fatigue Crack Initiation, Mechanics of Fatigue(ed. T.Mura), The Winter Annual Meeting of ASME, Nov.1981, pp.111-131
- /8/ T.Mura, Micromechanics of Defects in Solids, Martinus Nijhoff Publishers, 1982